# Hyper Spectral Image Characteristics of Aronia Melanocarpa Leaves under Saline Alkali Stress

**Yunfeng Ding[1] and Yanli Ma[2*]**

[1]College of Art and Design, Jilin Jianzhu University, Changchun 130118, China

[2]College of Landscape Architecture, Changchun University, Changchun 130012, China

*to whom all correspondence should be addressed: e-mail: 2175621875@qq.com

## GRPAHICAL ABSTRACT

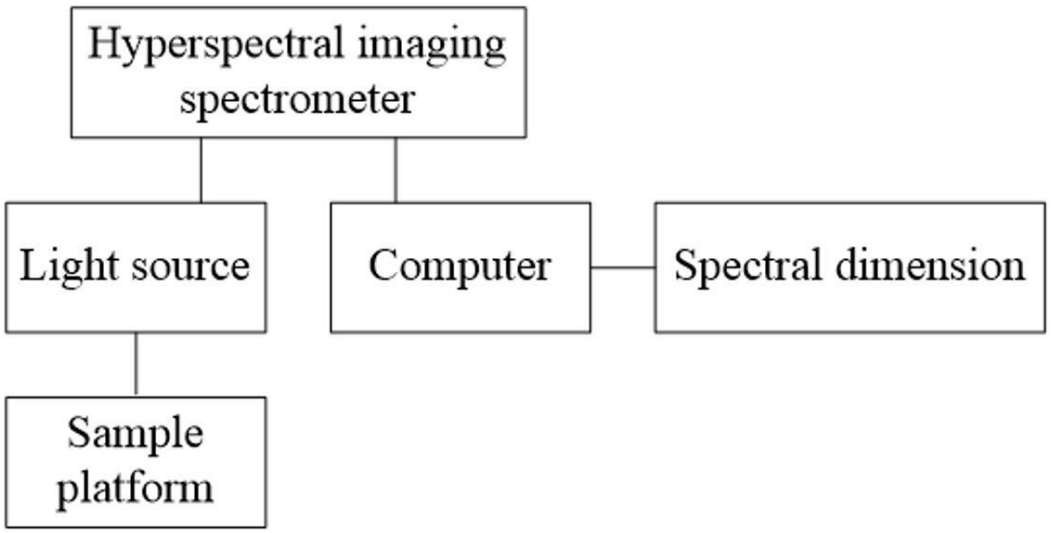


## ABSTRACT

Objective: To obtain the characteristics analysis results of aronia melanocarpa leaves under saline alkali stress state and improve yield and quality of aronia melanocarpa. Methods: Using hyper spectral imaging system to obtain hyper spectral images of aronia melanocarpa leaves under saline alkali stress. The clear hyper spectral image is obtained by the conversion of reflectance, spectral envelope removal, and spectral denoising, and final hyper spectral image is obtained by the normalization of a clearer hyper spectral image. Results: Spectral information of aronia melanocarpa leaves under slight saline alkali stress: in the visible band, leaf reflectance is lower than leaf nutrient rich stress condition; in the near infrared band, the nutrient rich leaves was significantly higher than that of stress leaves. Spectral information of leaves under moderate saline alkali stress: spectral reflectance of different lesion spots for a same leaf in 550-680nm band is: severe > moderate > slight > normal, in the near infrared band is on the contrary; spectral reflectance for different lesion grades in 550-680 nm, severe lesion leaves have highest reflectance, and normal leaves have the lowest reflectance. Under severe saline alkali stress, the leaf spectral information is: there is no significant difference in leaf spectral reflectance between the attachment aphid and the damaged leaf, but the difference is obvious for normal leaves in the band of 450-500 nm, 560-680 nm and 750-900 nm. Comparative results analysis for the three of saline alkali stress degree is: the near infrared band of 560-680 nm and the visible band of 780-900 nm is the sensitive band for the diagnosis of three kinds of stress; slight saline alkali stress has the most significant differences at 550 nm, and 780-900 nm; severe saline alkali stress has at 680 nm and 780-900 nm. Conclusion: The proposed method can analyze hyper spectral image characteristics of aronia melanocarpa leaves under different saline alkali stress the condition of is a kind of plant leaves, which is an efficient method for the analysis of characteristics of plant leaves under saline alkali stress.

**Keywords:** Aronia melanocarpa, Leaf, Saline Alkali stress, Hyper spectral image, Spectral reflectance, Photosynthetic pigment

## 1. Introduction

China is a great salt alkali country in the world, and unreasonable irrigation leads to more soil salinization. The high salinity and alkali content of soil will inhibit the growth of fruit trees and reduce the yield and quality of fruits (Kim and Lee, 2016). Many researches have been done on the development of fruit trees and saline alkali fruit resources in saline alkali soil, and great achievements have been made in saline alkali resistance mechanism, physiology and genetics of fruit trees. Aronia melanocarpa (Aronia melanocarpa Elliot) also known as wild cherry berry is a Rosaceae Aronia deciduous shrub, and native to the northeastern United States (Fu and Liu, 2017), (Ge et al., 2017), (Ogunkenle et al., 2019). It can be cultivated in three North Region of China with annual precipitation of >500 mm, extreme low temperature > -40°C, and soil pH<8.0 (Slavkovikj and Verstockt, 2016). Our country began to introduce it in 1990s. Aronia melanocarpa is a rare species in edible and medicinal, garden, and ecological value (Eriksson et al., 2018), (Ahamed et al., 2017), (Kim et al., 2018), (Grzeczka and Szymak, 2016). The fruit is rich in flavonoids, anthocyanins and polyphenols, aronia melanocarpa fruit and its extracts have good biological activity in antioxidant, anti-inflammatory, anti-cancer, lowering blood sugar, effects in the treatment of heart disease, hypertension and other cardiovascular and cerebrovascular diseases, which have broad prospects for development, but the relevant aronia melanocarpa salt tolerance physiological research has not been reported. The real data information on how to get the effective aronia melanocarpa under saline alkali stress condition has become a hot topic in recent years (Brzska and Rogalska, 2016), (D'Agata et al., 2020).

With the development of modern digital agriculture and the rapid updating of image measuring methods, spectral detection technology has the advantage of timely, fast and non-destructive, and it is applied to real-time monitoring and meticulous management of crop growth. Traditional crops are based on machine vision or spectral analysis technology for growth information diagnosis, which cannot provide surface continuous spectrum measurement and have many limitations (Varela and Fromentin, 2016), (Belbase et al., 2020). Because hyper spectral imaging has the advantage of map combination, it can be accurate to the point of a leaf to detect the characteristics of different stress symptoms of the crop and obtain the spectral information of the stressed crops. In recent years, some domestic and foreign scholars have successfully applied the hyper spectral imaging technology combining spectral detection and image detection to crop nutrient and disease stress diagnosis, and made preliminary progress (Ng et al., 2018). At present, scholars use quantitative hyper spectral imaging technology to extract all kinds of crops suffered stress characteristics, according to the analysis of local area high resolution images of the leaves, the suffer stress levels are ultimately determined, which makes the mechanism detection and research on a more micro scale (Arguello and Heras, 2015), (Sana et al., 2019). This study uses the hyper spectral imaging technology, with aronia melanocarpa as experimental material for an expansion experiments, that obtains reliable results and scientific, and provides effective analysis for aronia melanocarpa cultivation, production and utilization in our country.

## 2. Materials and Methods

### *2.1. Hyper Spectral Imaging Technology*

#### *2.1.1. Hyper spectral imaging system*

**Table 1.** Main performance indexes of spectrometers.

| Instrument model | Wavelength range | Spectral resolution | Accuracy | Sampling interval |
|---|---|---|---|---|

| | | | | |
|---|---|---|---|---|
| | | 3 nm (350 nm-1000 nm) | | 1.4 nm (350 nm-1000 nm) |
| Push scavenging imaging spectrometer PIS | 350 nm-2500 nm | 8.5 nm (1000 nm-1900 nm) | +/-1 nm | 2 nm (1000 nm-2500 nm) |
| | | 6.5 nm (1700 nm-2500 nm) | | |

The working process of the system is shown in Figure 1. The system is composed of pushbroom imaging spectrometer (PIS), electrically controlled translation platform and controller, adjustable halogen light source, desktop computer and other components (Qi and Zhao, 2014), (Cyril, 2019). Before the use of the spectrometer, the national optical radiation calibration and sign Technology Innovation Laboratory of the Anhui Institute of Optics and fine mechanics of Chinese Academy of Sciences was commissioned to strictly test and calibrate the spectrometer (Kwon and Kang, 2016), (Augustine and Marlia, 2019). The effective spectrum acquisition range of the instrument is 350 nm-2500 nm, and its detailed parameters are shown in Table 1. Other technical parameters of the spectrometer include: the number of sampling times per second is 10 times; the accuracy of wavelength acquisition is within 1 nm; when the temperature changes in 10 degrees, the repeatability of wavelength can be controlled within 0.3 nm. The spectral resolution of spectrometer in different wavelength and sampling interval is not the same, when the wavelength is between 1700 nm-2500 nm, the spectral resolution is 6.5 nm (Liu and Liu, 2010), (Nkwuda et al., 2019) when the wavelength in the range of 1000 nm-1900 nm, the spectral resolution is 8.5 nm; when the wavelength is between 350 nm-1000 nm, the spectral resolution is 3 nm; and when the wavelength interval is 350 nm-1050 nm, the sampling interval is 1.4 nm; when the wavelength interval is within 1050 nm-2500 nm, the spectral sampling interval is 2 nm. When the whole spectral curve is collected in the effective interval of 350 nm-2500 nm, the instrument will automatically resample the collected curves, and output the spectral characteristic curves of 350 nm-2500 nm in the effective band. The spectral interval is 1nm, and there are 2151 effective bands.

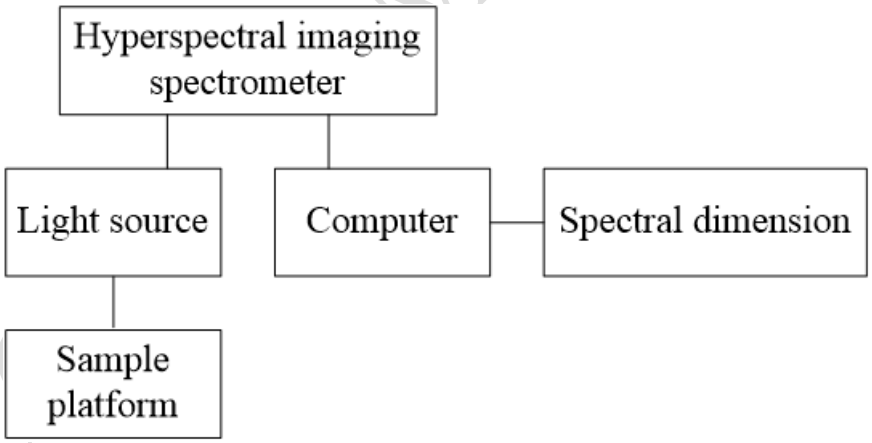


**Figure 1.** Demonstration of hyper spectral imaging system.

*2.1.2. Imaging spectrum acquisition and reflectance conversion*

Before the hyper spectral imaging of the leaves, the height of the instrument is fixed according to the imaging effect. The measured lens is 380 mm away from the electric translation platform, and the light source is 45 degrees from the platform to 300 mm. The suitable speed of the electric translation platform is 2.3 $mm \cdot s^{-1}$. Then the parameters of the imaging acquisition system are set up, the best exposure time and frame frequency are 100 ms and 9 FTPS, respectively (Kang et al., 2018), (Butt et al., 2020). Aronia melanocarpa leaves tile in black cloth, and the reference plate is placed in the field of reference spectrometer. As the electric moving platform moves at a constant speed, the hyper spectral cubes of the leaves and the reference plate are obtained simultaneously. Among them, each picture contains 1024 spectral bands. The hyper spectral images collected in the BMP format are stored in the computer. In

order to extract and analyze the spectral features of the data, we need to complete the mosaic and reflectance conversion of the spectral images (Majdar and Ghassemian, 2017). The purpose of the logarithmic transformation (log (I/R)) of the reciprocal of spectral reflectance is to enhance the spectral difference value of the lower reflectivity (Brzska and Tomczyk, 2015). Comparing the original spectral reflectance curve, aronia melanocarpa leaves generally has low spectral reflectance in the visible band, and the band is the reflection and absorption of leaves with pigment (Appice and Guccione, 2016). Therefore, the reciprocal logarithmic transformation of the original spectral reflectance can effectively enhance the spectral difference of these bands, and at the same time, it can also weaken the random error caused by different illumination (Goh and Youn, 2016). Spectral reflectance curve of the logarithm of reciprocal transformation is represented in Fig. 2. In this paper, the original image is spliced into BIL format of the whole image by MATLAB7.0 software, and then the reflectance transformation of image is completed by using the empirical linear method module with ENVI4.5 software.

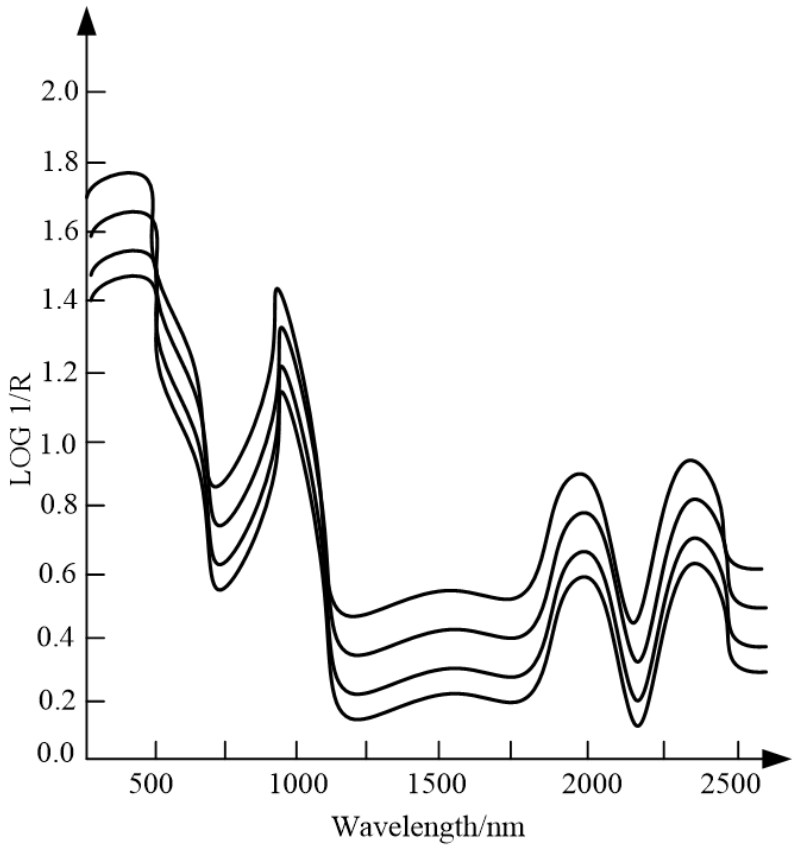


**Figure 2.** After logarithmic transformation of spectral inverse.

Fig. 2 showed that the logarithmic transformation of the spectral reciprocal is equivalent to the local stretching enhancement of the low reflectivity of the original spectrum, although some spectral features are highlighted, the overall effect is not obvious, which can be proved by the results of subsequent correlation analysis.

*2.1.3. Spectral envelope removal transformation*

In order to enlarge the spectral characteristics of spectral images and show better spectral information and features, the envelope removal of spectral images after reflectance transformation is completed (Zhang and Zhu, 2012). The continuum removal (CR) of spectral envelope was first discovered by Clark and Roush to suppress the background values in the spectral data and enhance small and easily lost reflection peaks and absorption valleys in enhanced spectral curves, which can effectively increase the

spectral signal-to-noise ratio of the data and highlights the spectral characteristic information (D 'Alessandro and Dimitrov, 2014). The spectral envelope removal conversion is shown as Formula (1).

$$R'(\lambda)=\frac{R(\lambda)}{R_c(\lambda)} \quad (1)$$

In Formula (1), $R(\lambda)$ represents the original spectral reflectance value at $\lambda$, $R'(\lambda)$ represents the spectral reflectance envelope at $\lambda$ band and the value of transformation is removed (Singh and Raj, 2019). $R_c(\lambda)$ represents the mean value of reflectivity of continuum in band $\lambda$. Fig. 3 describes the curve after the envelope is removed. Compared with the original spectral reflectance, spectral characteristics of continuum removal transform can effectively enlarge the spectral curve (Zhou and Wei, 2016) and contribute to the extraction of aronia melanocarpa plant spectral sensitivity band information.

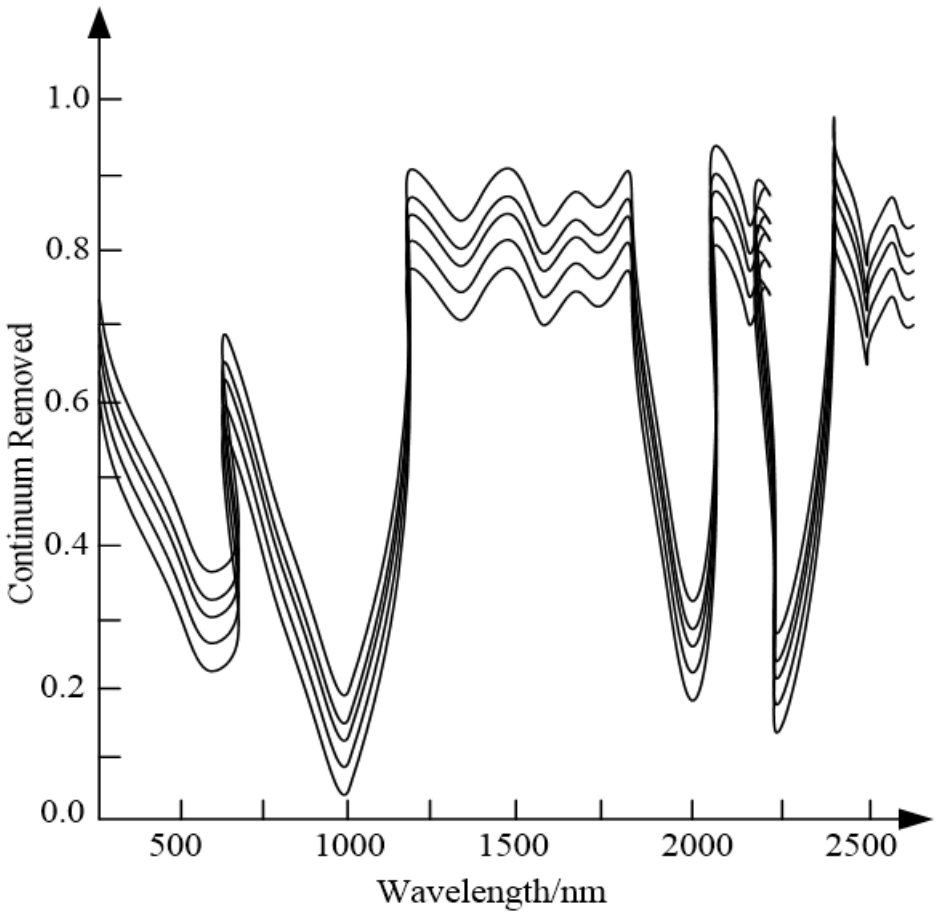


**Figure 3.** Envelope removals after transformation curve.

*2.1.4. Spectral feature enhancement*

Because the dark current of the spectrometer is not uniform in response to each band, the image contains noise (Tang and Gao, 2016). This paper uses the S-G convolution smoothing module in Origin7.5 software for spectral denoising and spectral curve expression (Bao, 2017). At the same time, in order to get rid of the need of study, the noise band was removed, and the final used effective band is 450-900 nm. In order to enhance the spectral characteristics of leaves under different saline alkali stresses and eliminate the difference of reflectance caused by illumination, the reflectivity is normalized by normalization method (Szopa and Ekiert, 2014). Its principle is to calculate the spectral mean of each

pixel, and the spectral reflectance of each band is then divided by the mean, as shown in Formula (2). The final normalized reflectance is between 0 to 25.

$$R_{ij} = \frac{R_{ij}}{\left(\frac{1}{K}\sum_{j} R_{ij}\right)} \tag{2}$$

$R_{ij}$ represents normalized reflectivity, $i$ and $j$ represent initial and terminating bands, and $K$ represents the total number of bands. The images after the normalization are analyzed.

## 3. Results

### *3.1. Extraction and analysis of spectral features for aronia melanocarpa leaves under slight saline alkali stress*

In this study, the results obtained by the experiments are made into a curve diagram, as shown in Fig. 4, which describes the spectral reflectance of aronia melanocarpa leaves under three condition saline alkali stresses of slight, moderate and severe. According to the crop growth rule, the nutrient of the aronia melanocarpa leaves of different leaf positions is different under the saline alkali stress, and the spectral information are different at the same time. In this study, the spectral information of different leaf positions is extracted from the hyper spectral images of leaves. As shown in Fig. 5 (a), the reflectance of different levels of leaves is shown in Fig. 5 (b).

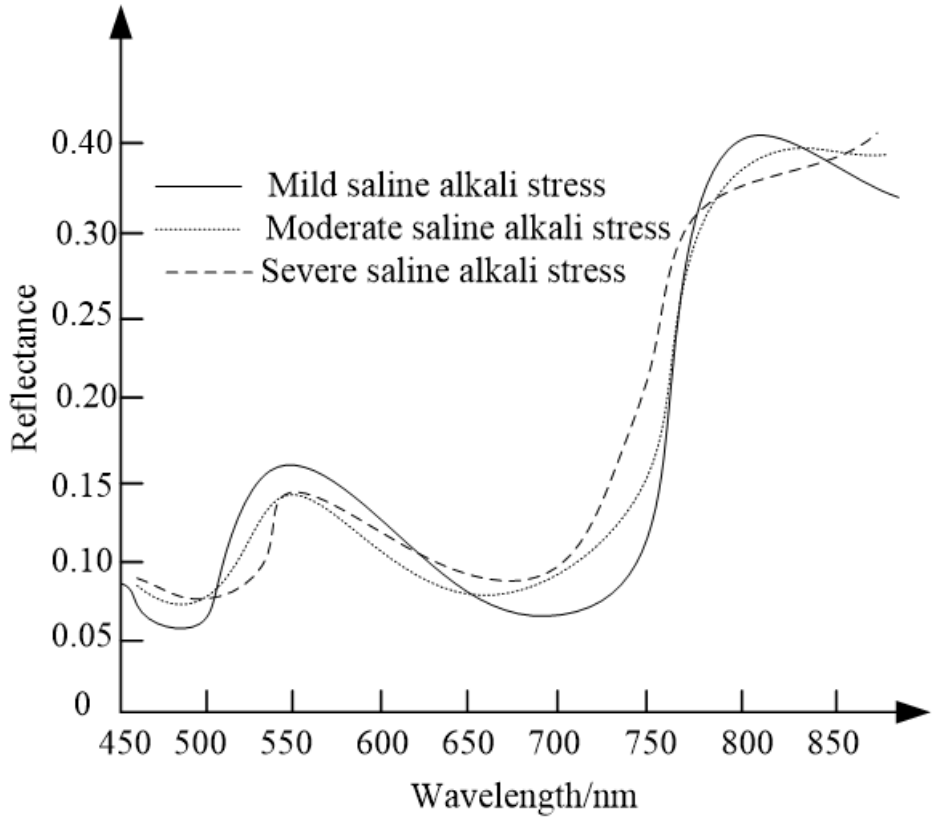


**Figure 4.** Spectral reflectance of leaves under different saline alkali stress.

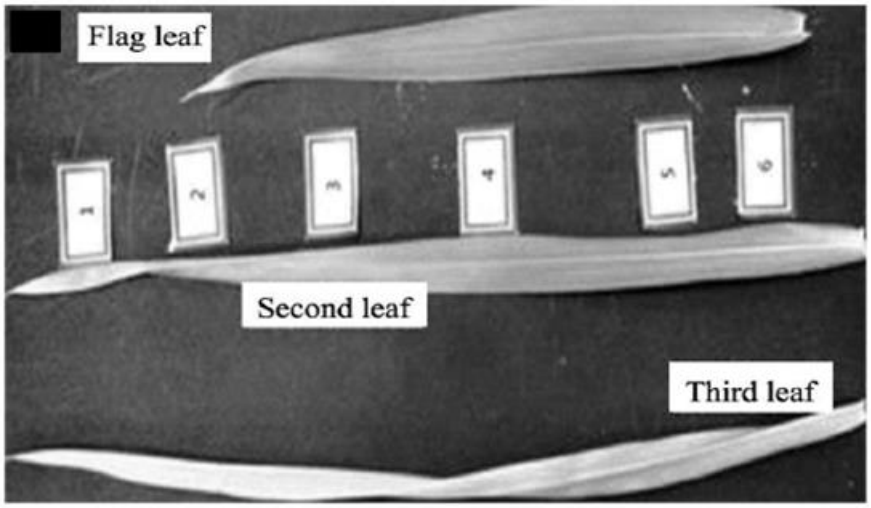


(a) Imaging of different layers of leaves

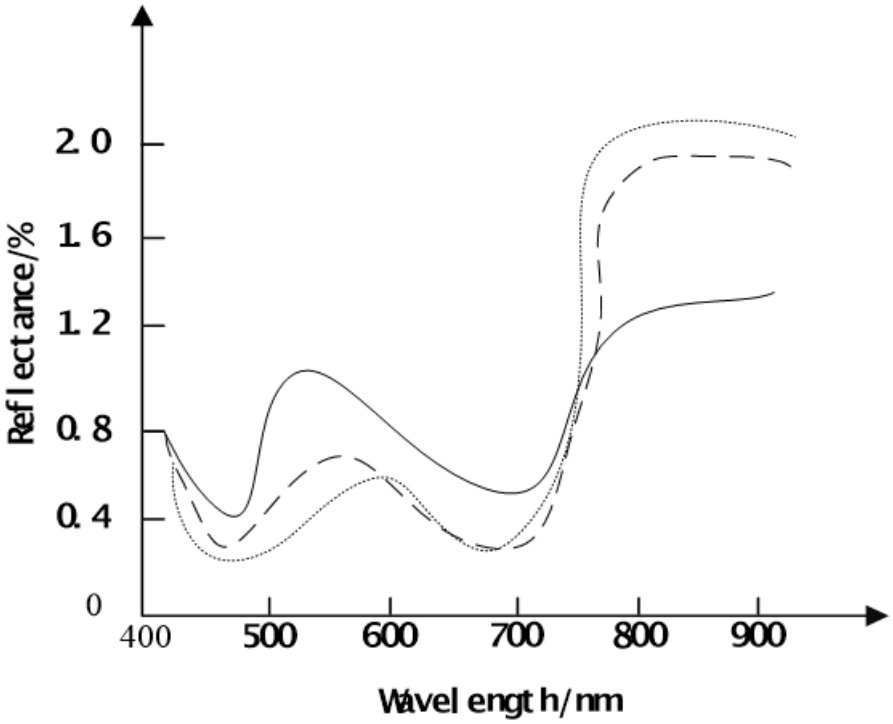


(b) Albedo of different levels of leaves

**Figure 5.** (a)Imaging of different layers of leaves(b)Albedo of different levels of leaves.

### *3.2. Extraction and analysis of spectral features for aronia melanocarpa leaves under moderate saline alkali stress*

Because of the high spectral cube of aronia melanocarpa leaves contains two-dimensional map information, each pixel on the image are continuous spectral information in the range, the crops suffered from qualitative and quantitative saline alkali stress has a unique advantage analysis. Aronia melanocarpa will have a certain number of leaf spots in moderate saline alkali stress condition; this study uses characteristics of imaging spectrometer with high spatial resolution in the near earth observations, quantitatively studied the effects of moderate salt stress on the number of leaves and the area of infection (Algarni, 2019). The number and the features of spots in the same leaf was studied firstly, as shown in Fig. 6, then the leaf lesion severity was qualitatively researched as shown in Fig. 7.

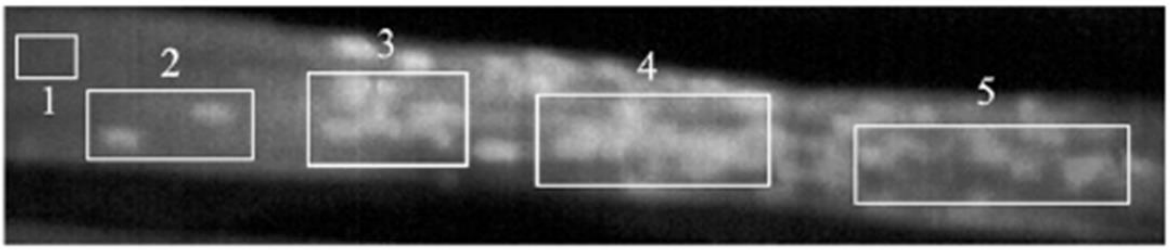


1:0%；2:5%；3:15%；4:3%；5:50%；

**Figure 6.** Single leaves on a different number of spots.

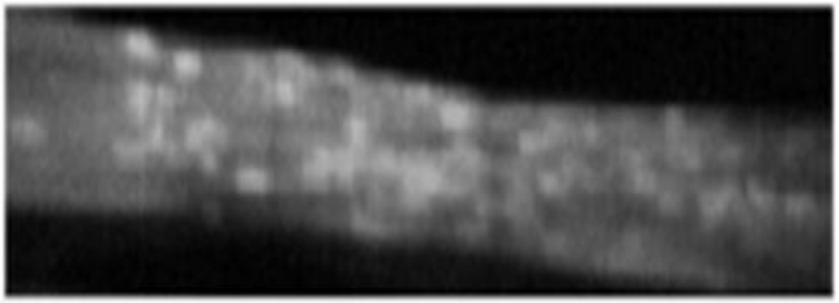

(a) 3 level, severe

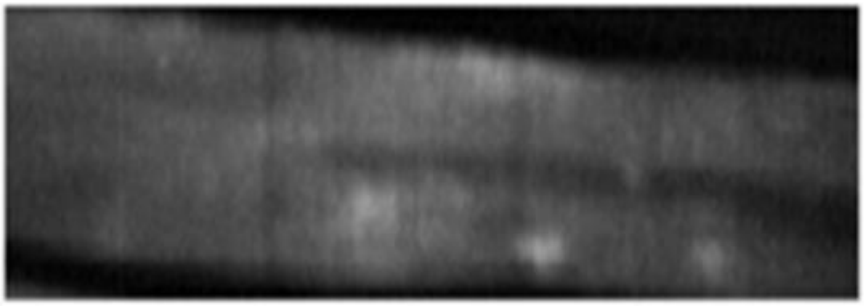

(b) 2 level, moderate

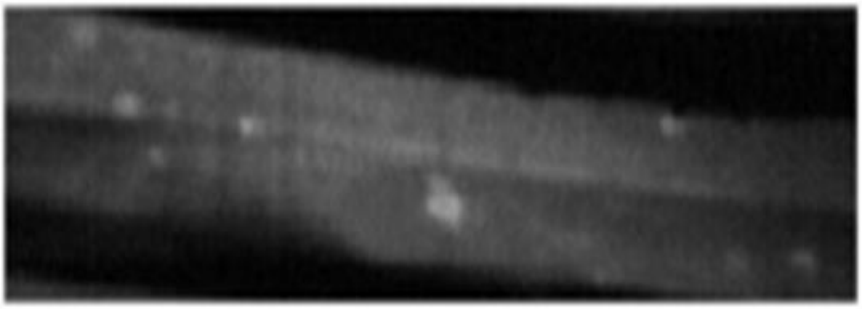

(c) 1 level, slight

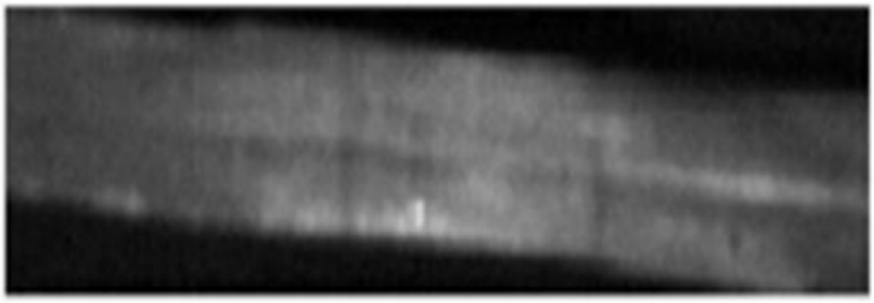

(d) 0 level, normal

(a) Severe (b) Moderate (c) Slight (d) Normal

**Figure 7.** The different degree of leaf spot disease.

Fig. 8 is a leaf reflectance of different lesion number and different grades of leaf spots in 450-900 nm band. Comparative analysis of spectrum and lesion around the normal part of the lesion was shown in Fig. 8(a), the difference of spectral information with the whole leaf spot was shown in Fig. 8(b).

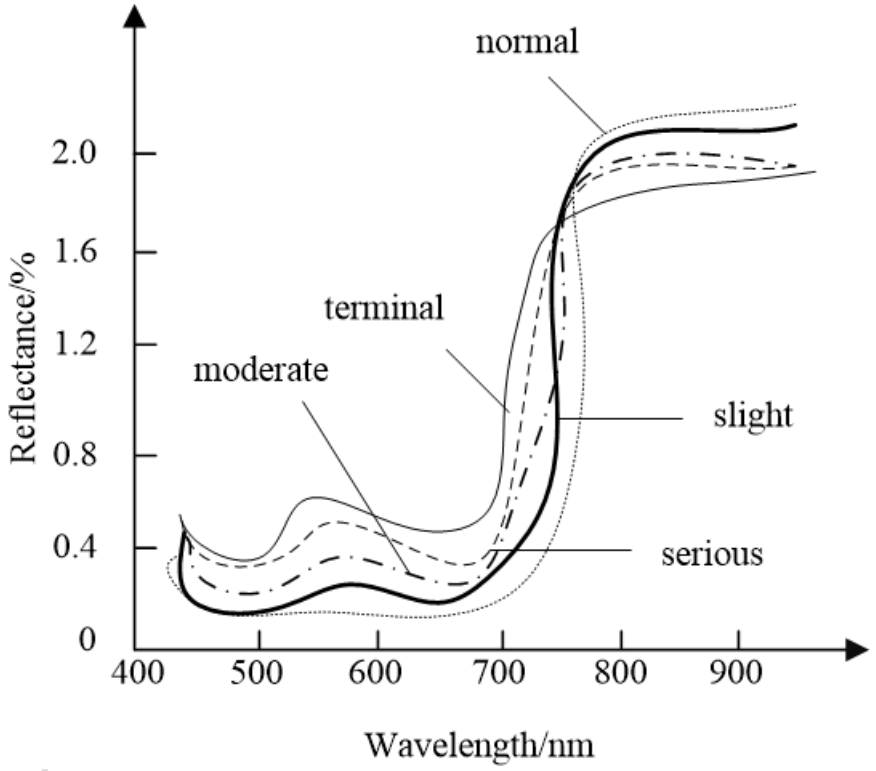


(a) Around the lesion spectrum and normal part of the spectrum of the lesion.

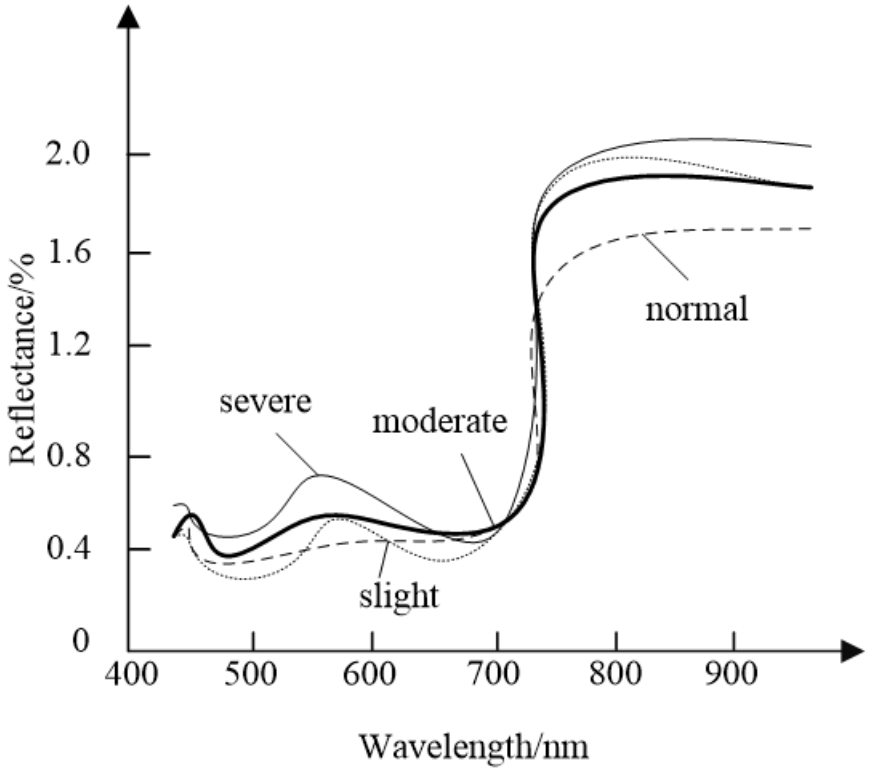


(b) The difference of spectral information with the whole leaf spot.

**Figure 8.** Leaf hyper spectral reflectance lesions.

*3.3. Extraction and analysis of spectral features for aronia melanocarpa leaves under severe saline alkali stress*

Aronia melanocarpa leaves in severe saline alkali stress state will attract a large number of aphid damage on the leaves, the imaging spectrometer used in this study can be accurate to 0.5 mm, in the acquisition of planar leaf spectral images, the analysis of aphid number and population spectrum can be extracted, which provides a new means for the quantitative study of the aronia melanocarpa leaves harms under severe saline alkali stress. The albedo of the aphis leaves, the reflectivity of the destructive leaves, the reflectivity of the normal leaves and the albedo of the aphids were described in detail in Fig. 9. Figure 10 describes the leaves of the aphid and the leaves without aphids.

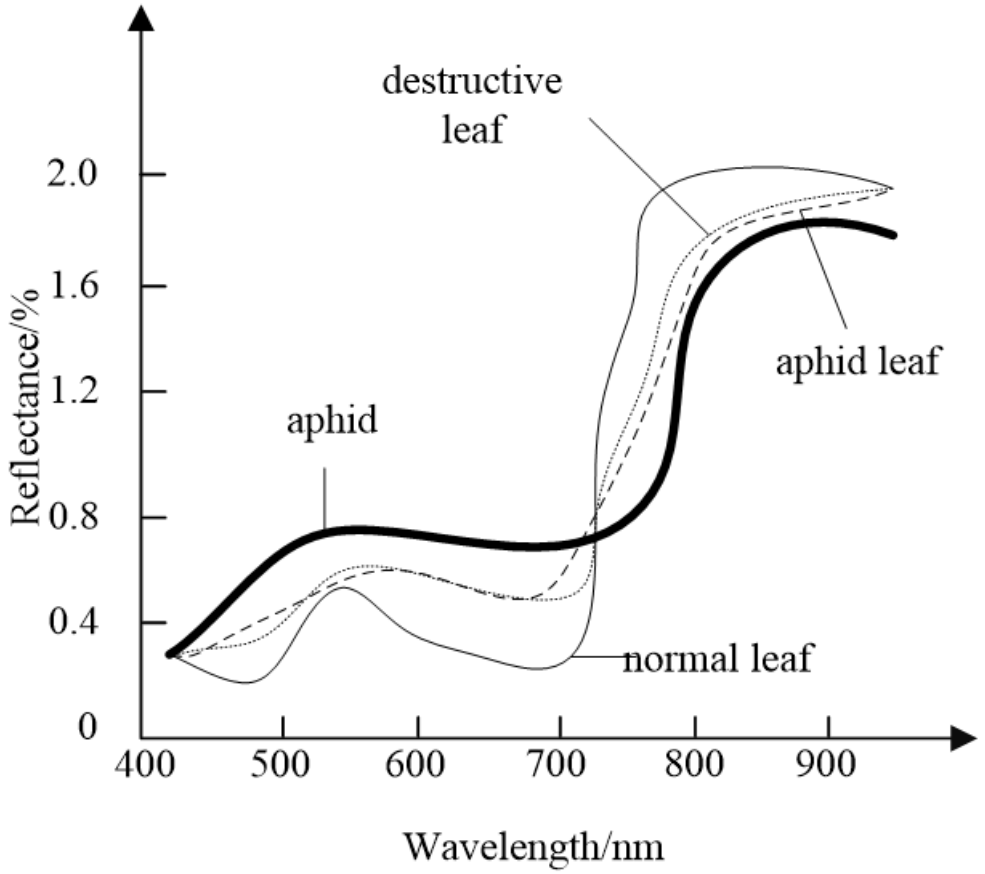


**Figure 9.** Albedo of Aphis leaves, reflectivity of destructive leaves, reflectivity of normal leaves, and albedo of aphids.

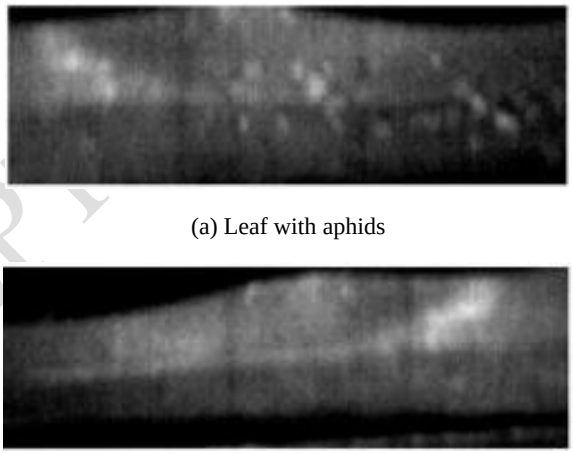

(a) Leaf with aphids

(b) Leaf of removing aphids

**Figure 10.** (a): Leaf with aphids；(b): Leaf of removing aphids.

*3.4. Effects of three saline alkali stress on chokeberry leaf free water and bound water content*

Aronia melanocarpa leaves were processed with the proposed method, the data of free water and bound water content obtained in the leaves were made into curves, as shown in Fig. 11.

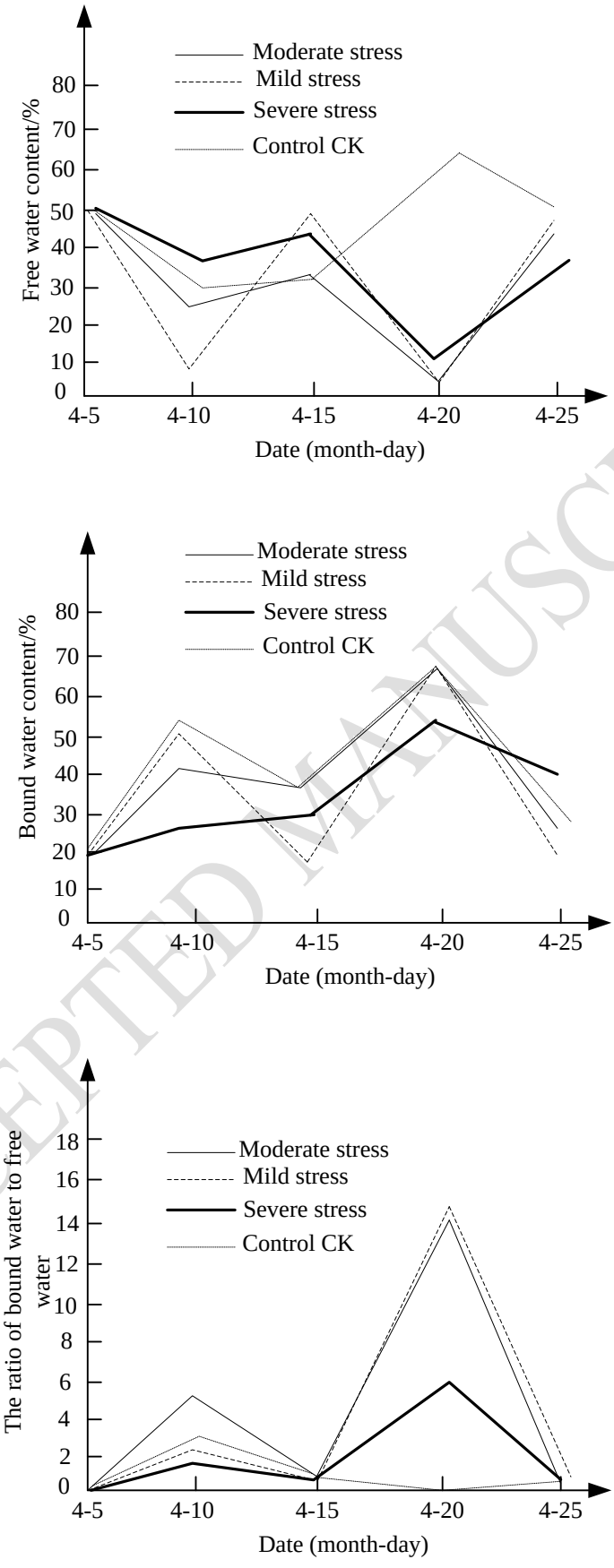


**Figure 11.** Effects of three saline alkali stress on chokeberry leaf free water and bound water content.

*3.5. Effects of three saline alkali stress on chokeberry leaf photosynthetic pigment content*

The photosynthetic pigments of aronia melanocarpa leave in this study including chlorophyll a, chlorophyll b and carotenoid content. Aronia melanocarpa leaves were processed with the proposed method, the aronia melanocarpa chlorophyll a, chlorophyll b and carotenoid content related data information were made into curves, as shown in Fig. 12.

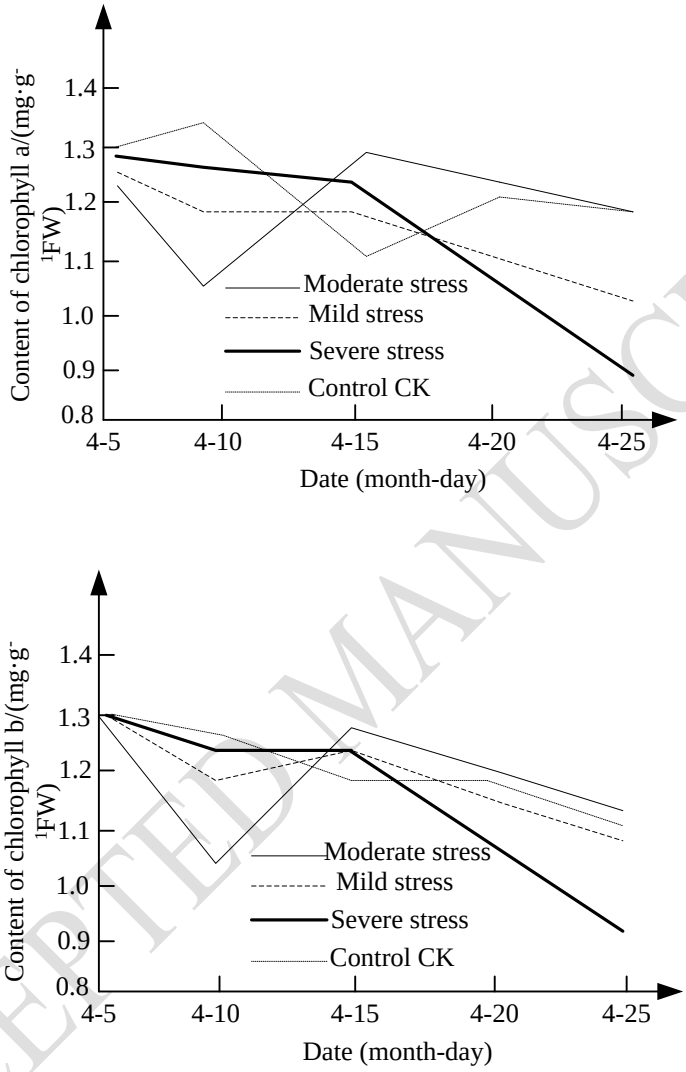

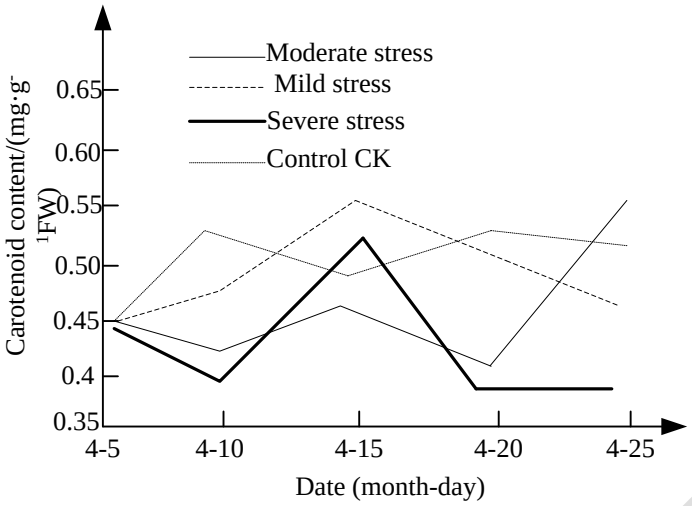


**Figure 12.** Effects of three saline alkali stress on chokeberry leaf photosynthetic pigment content.

## 4. Discussion

*4.1. Spectral feature discussion of aronia melanocarpa leaves under slight saline alkali stress*

Fig. 5 (a) describes the imaging of different layers of leaves. The purpose is to eliminate the spot data errors caused by uneven illumination distribution, and to explore the spectral difference caused by nutrient loss more accurately on the vertical gradient of crops. Fig. 5 (b) showed that in the visible band, reflectivity of the lower layer is the highest, the middle level is lower, and the upper layer is the lowest, especially in the red and green band of 550-650 nm; secondly, the absorption valley is found near 680 nm, and the lower and upper middle levels are different; the band of 700-760 nm has the red edge characteristics of vegetation characteristic, in the upper leaves, the upper and middle leaves are in good condition, so the red shift, while the lower leaves for nutrient deficiency and yellow, red edge moves towards the blue wave. The main reason for the difference of the spectral characteristics is that the content of chlorophyll in the leaves is different. This is consistent with previous studies. Chlorophyll content is a sensitive factor of the analytical spectral change. The visible light band is characterized by chlorophyll a, the strong reflection of the chlorophyll b in the blue and green light region and the strong absorption of the red light region.

The near infrared band of 780-900 nm is the opposite of the visible light band. The upper and upper middle leaves are strong with vitality, the cell structure is perfect, and the light is scattered in the leaves, so the reflectivity is high; while the lower layer is yellow, the content of chlorophyll is reduced, the cell structure changes, and the reflectivity of the lower layer is obviously lower than that of the middle and upper middle layer. This is in accordance with the research results of other scholars under different fertilization treatments. That is, the difference of the multiple scattering caused by the structure of the leaf cell is the criterion for the near infrared band.

According to the results of the extraction and analysis of spectral characteristics under slight saline alkali stress, this study used hyper spectral imaging technique for the saline alkali stress diagnosis of leaves in different leaf positions, high spectral differences can be extracted in different position leaves, it also provides a means for accurate diagnosis of crop nutrient stress according to the imaging of intuitive visual judgment.

*4.2. Spectral feature discussion of aronia melanocarpa leaves under moderate saline alkali stress*

Through the description of Figure 6 and Figure, it can give full play to the advantages of an imaging spectrometer, extract spectral features extracted from diseased leaves in two dimensions, and investigate the different lesion degree of leaf spectra from the microscopic response.

Fig. 8 can comprehensively reflect the spectral characteristics of leaf lesion under moderate saline alkali stress. Fig. 8 (a) shows that in 550-680 nm wavelength range, the leaf reflectance of different lesion showed the rules that serious (50%) > severe (30%) > moderate (15%)> slight (5%) > normal (0%). This is because in the visible light band, the spectral properties of the crops are mainly influenced by the content of chlorophyll. The normal leaf appears the 550 nm reflection peak and the 680 nm absorption valley. When leaf lesion was caused by moderate saline alkali stress, the chlorophyll content decreased, visual performance is light yellow and white, the absorption value decreased in the sunlight, so the reflection is higher. In the near infrared band of 780-900 nm, the spectral reflectance of the normal part of the leaf and the part of the lesion has obvious difference. The general rule was normal (0%) > slight (5%) > moderate (15%) > severe (30%) > serious (50%), which was the opposite of visible light. This is because the spectral characteristics of leaves in the near infrared band is determined by the internal structure of leaf cells, normal aronia melanocarpa leaf cells makes multiple scattering of light, so the reflectivity is high, and the leaf spot effect on the internal structure of the leaves, so the reflectivity value is low. Fig. 8 (b) shows that the bands of 550-680 nm and 780-900 nm are still sensitive bands for judging different grades of disease; the number of rules and the spot number of single leaf are consistent. However, the analysis of the reflectance shows that the visible light band is significantly different from the near infrared band; spectral differences between normal and severe leaves were obvious; but the spectrum of slight and moderate disease was not significantly different. It shows that there is a certain error when the point form spectral data reflect the surface information. So to truly detect impact of disease on leaves, it should consider the percentage of lesion number, size and proportion of leaves, otherwise it will lead to the establishment of the representative model reduction.

*4.3. Spectral feature discussion of aronia melanocarpa leaves under severe saline alkali stress*

From Fig. 9, we can see that the reflectivity curves of four states have the same trend, that is, the reflection peak of 550 nm, the absorption valley of 680 nm, the red edge of 680-780 nm, and the near-infrared reflector platform after 780 nm. However, the red light band of normal leaves at 680 nm had the most significant absorption valley, the leaves attached and damaged by aphids take the second place, and the aphids also had a similar spectrum. The reflectance values of the normal leaves in the near infrared range were the highest, followed by the leaves with damaged leaves and aphids. It shows that the normal cell structure in the normal leaf is normal and forms multiple reflections, so the reflection value is the highest. The albedo of aphids increased gradually with the increase of the band, but it was lower than the reflectance of the leaves before and after the insect pests. The reflectance of leaves of normal leaves and aphids is different from 450 to 500 nm, 560 to 680 nm, and 750 to 900 nm bands, which can be used as an identification band to judge the aphid stress. The leaf albedo of the aphids and the leaves damaged by the aphids were not very different. The two were called the stress state of the crops. In the 450-700 nm band, aphids reflectance was the highest, but also showed the reflection peak of 550 nm, and the absorption peak of 680 nm, which showed that the aronia melanocarpa leaves more or less have certain contribution; but in the red edge position of 700-780 nm, it is obviously different from the spectral characteristics of green plants, so we can put the red edge in order to determine characteristics of regional aphid disease leaf caused by alkali stress.

*4.4. Change of aronia melanocarpa leaves biomembrane stability under saline alkali stress*

The stability of the structure and function of the biomembrane is closely related to the resistance of the plant. Saline alkali stress caused damage to the cell membrane, causing a large exodus of osmotic substances, and result in a rise in electrical conductivity. The results of this study is from slight to severe saline alkali stress treatment, relative conductance of the leaf is increased gradually, but the slight stress saline alkali treatment have little effect on the leaf cell membrane permeability.

The content of MDA on behalf of the plant membrane lipid peroxidation level, which reflects the injury extent of the aronia melanocarpa leaves. A lot of researches reported the increasing level of MDA in aronia melanocarpa leaves under saline alkali stress. The experimental results showed that with increasing salt concentration and alkali treatment time, MDA content in aronia melanocarpa leaves is gradually increased, and the degree of injury of aronia melanocarpa is greater. But when the aronia melanocarpa leaves were in slight saline alkali stress, leaf MDA content was not significantly increased, and the control tends to be consistent, which confirms the relevant aronia melanocarpa cell membrane permeability of the conclusion, once again proved that aronia melanocarpa has certain salt resistance ability. At the same time, the test results showed that although aronia melanocarpa has certain salt resistant ability, it does not prove that aronia melanocarpa salt resistance ability is how strong, because the saline water irrigated with different concentrations in this experiment, with the increase of irrigation times, soil nutrition in salt alkali would gradually accumulate, salt concentration will continue to increase, but the changes in the amount of salt and alkali in the nutrient soil are not measured in the experiment. In order to solve this problem, we should prepare different saline alkali soil salinity, and determine the concrete salt resistance ability through the observation of aronia melanocarpa in different saline alkali soils, so as to more effectively guide the production of aronia melanocarpa.

## 5. Conclusions

In this paper, spectral feature based on hyper spectral imaging technology of aronia melanocarpa leaves in different saline alkali stress were extracted and analyzed. There are the following conclusions.

(1) Aronia melanocarpa leaves in slight saline alkali stress, leaf spectral information is: in the visible band, the leaf reflectivity of nutrient sufficient leaves is lower than that under stress; in the near infrared band, the leaf reflectivity of nutrient sufficient leaf was obviously higher than the stressed leaf. This provides a theoretical basis for the study of nutrient diagnosis at different levels of crops from the perspective of hyper spectral image technology.

(2) Leaf spots of aronia melanocarpa leaves were caused by moderate saline alkali stress, spectral reflectance of different leaf lesion in 550-680 nm is serious > severe > moderate > slight > normal, which is on the contrary in the near infrared band. However, different spectral grade lesion leaf reflectance at 550-680 nm was that the reflectance was highest when lesion was severe; the normal leaf reflectance was the lowest; difference between slight and severe was not obvious. In the near infrared band, the result is opposite and the difference between the different levels of the lesion is not obvious. In addition, the obtained spectral data reflect the planar information point has some error. To comprehensively reflect the real situation, we need to consider the leaf lesion size, lesion number, total leaf area and other factors, otherwise it will affect the accuracy of the model.

(3) Aronia melanocarpa leaves in severe saline alkali stress leads to erosion of leaves by aphids, spectral reflectance difference of leaves attached and damaged by aphid were not obvious, but differences of normal leaves were significant at bands of 450-500 nm, 560-680 nm and 750-900 nm; aphids also showed the spectral reflectance characteristics of vegetation to some extent, but the overall was high, and that in the red edge and near-infrared bands is obviously low, which can be used as a division of severe saline alkali stress index to provide a reference.

(4) It showed that aronia melanocarpa has certain anti salt ability through the photosynthetic pigment content analysis, black fruit gland rib of flowers; carotenoid content of aronia melanocarpa leaves greatly influenced by salt and alkali stress, the long-term saline alkali stress can decrease the carotenoid content of leaves significantly, but if the saline alkali stress is slight or short-time, the carotenoid content will increase, so as to reduce the stress of harm, it also showed that aronia melanocarpa has a certain ability to adapt to saline alkali stress.

(5) The more MDA content in aronia melanocarpa leaves, the larger degree of injury to the plant is. But in slight saline alkali stress, aronia melanocarpa leaf MDA content was not significantly increased,

which confirms the conclusion of the relevant aronia melanocarpa cell membrane permeability, which once again proved that aronia melanocarpa has certain salt resistance ability.

In order to make aronia melanocarpa adapt to saline alkali stress environment, and grow better under stress conditions, the following three methods can be used to improve the salt tolerance of aronia melanocarpa:

(1) Seed treatment: Seed treatment is usually before planting with inorganic or organic matter soaking, high or low temperature treatment, seed priming techniques to preprocess the seeds which can improve the seed vigor and germination rate, is conducive to the accumulation of ions and compounds during germination, and to better adapt to the saline alkali habitat.

(2) Exogenous compounds: Usually in planting after applying inorganic or organic compounds such as growth regulators, it is to improve the content of plant essential elements and trace elements in the body, to enhance photosynthetic capacity, reduce the activity of antioxidant enzymes, maintain cell membrane permeability and ion balance, so as to alleviate salt stress damage to the plant, and improve plant salt tolerance. The commonly used inorganic substances includes $Ca(NO_3)_2$, $KNO_3$, $K_2SO_4$, Si, etc. Commonly used growth regulators include gibberellin and abscisic acid.

(3) Breeding salt tolerant varieties: It contains selection, breeding, selection of mutants, transgenic and tissue culture from varieties, etc.

**Authors' Contributions**

Yunfeng Ding: Modelling and optimization, writing of manuscript;

Yanli Ma: Proposal of the research topic, experiments,modelling, writing of manuscript.

**References**

Ahamed, A. J., Loganathan K., Ananthakrishnan S., Ahmed J., and Ashraf M. A. (2017). Evaluation of graphical and multivariate statistical methods for classification and evaluation of groundwater in alathur block, perambalur district, india. *Applied Ecology and Environmental Research*. **15**, 105-116.

Algarni, S. (2019). Potential for cooling load reduction in residential buildings using cool roofs in the harsh climate of Saudi Arabia. *Energy & Environment*. **30**, 235-253.

Appice, A., P. Guccione, and D. Malerba. (2016). Transductive hyper spectral image classification: toward integrating spectral and relational features via an iterative ensemble system. *Machine Learning*. **103**, 343-375.

Argüello, F., and D. B. Heras. (2015). ELM-based spectral–spatial classification of hyper spectral images using extended morphological profiles and composite feature mappings. *International Journal of Remote Sensing*. **36**, 645-664.

Augustine EE, Marlia MH (2019). Awareness Level of Water Resource Conservation of University Students. *Water Conservation and Management*, **3,** 18-21.

Bao, Q. (2017). Simulation Research for Spectral Image Chinese native medicine ingredient content detection. *Computer Simulation*. **34**, 369-372.

Belbase S, Tiwari A, Baral S, Banjade S, Pandey D (2020). Study Of Improved Mandarin (Citrus Reticulate Blanco) Orchardmanagement Practices In Mid Hills Of Gandaki Province, Nepal. *Malaysian Journal of Sustainable Agriculture*, **4,** 49-53.

Brzóska, M. M., J. Rogalska, and A. Roszczenko, et al. (2016). The mechanism of the osteoprotective action of a polyphenol-rich aronia melanocarpa extract during chronic exposure to cadmium is mediated by the oxidative defense system. *Planta Medica*. **82**, 621-631.

Brzóska, M. M., M. Tomczyk, and J. Rogalska, et al. (2015). Protective impact of extract from Aronia melanocarpa berries against low-level exposure to cadmium-induced lipid peroxidation in the bone tissue: a study in a rat model. *Planta Medica*. **81**, 247-8.

Butt A, Umer S, Altaf R (2020). Performance Of Two Hybrids Of Helianthus Annuus L. (Sunflower) Under The Stress Of Heavy Metals I.E. Zinc And Copper. *Journal Clean Was*, **4,** 08-11.

Cyril C. O (2019). High Resolution Magnetic Field Signatures Over Akure And Its Environs, Southwestern Nigeria. *Earth Sciences Malaysia*, **3,** 09-17.

D'Agata C., Diolaiuti G., Maragno D., Smiraglia C. & Pelfini M. (2020) Climate change effects on landscape and environment in glacierized Alpine areas: retreating glaciers and enlarging forelands in the Bernina group (Italy) in the period 1954–2007, *Geology, Ecology, and Landscapes*, **4,** 71-86.

D'Alessandro, L. G., K. Dimitrov, and P. Vauchel, et al. (2014). Kinetics of ultrasound assisted extraction of anthocyanins from Aronia melanocarpa (black chokeberry) wastes. *Chemical Engineering Research & Design*. **92**, 1818-1826.

Eriksson, M., R. Ghosh, E. Hansson, S. Basnet, and C. Lagerkvist. (2018). Environmental consequences of introducing genetically modified soy feed in Sweden. *Journal of Cleaner Production*. 176:46-53.

Fu, H., and X. Liu. 2017. Research on the Phenomenon of Chinese residents' spiritual contagion for the reuse of recycled water based on SC-IAT. *WATER*. **9**(84611)

Ge, S., Z. Liu, Y. Furuta, and W. Peng. (2017). Adsorption characteristics of sulfur solution by acticarbon against drinking-water toxicosis. *Saudi Journal of Biological Sciences*. **24**, 1355-1360.

Goh, A. R., G. S. Youn, and K. Y. Yoo, et al. (2016). Aronia Melanocarpa Concentrate Ameliorates Pro-Inflammatory Responses in HaCaT Keratinocytes and 12-O-Tetradecanoylphorbol-13-Acetate-Induced Ear Edema in Mice. *Journal of Medicinal Food*. **19**, 654.

Grzeczka, G., and P. Szymak. (2016). The hardware implementation of demonstrator air independent electric supply system based on pem fuel cell. *Polish Maritime Research*. **23**, 84-92.

Kang, L., H. L. Du, X. Du, H. T. Wang, W. L. Ma, M. L. Wang, and F. B. Zhang. (2018). Study on dye wastewater treatment of tunable conductivity solid-waste-based composite cementitious material catalyst. *Desalination and Water Treatment*. **125**, 296-301.

Kim, N. Y., and H. Y. Lee. (2016). Enhancement of cognitive functions by aronia melanocarpa elliot through an intermittent ultrasonication extraction process. *Journal of Medicinal Food*. **19**, 245-252.

Kim, N. Y., E. J. Jeon, S. H. Jung, S. J. Ahn, M. A. Park, and J. S. Seo. (2018). Gene expression profiling and expression analysis of freshwater shrimp (Neocaridina denticulata denticulata) using expressed sequence tags and short-term exposure to copper. *Journal of Environmental Biology*. **39**, 51-57.

Kwon, J. H., D. W. Kang, and S. Y. Lee, et al. (2016). First report of brown leaf spot caused by Alternaria alternata on Aronia melanocarpa in Korea. *Plant Disease*. **100**, 1011-1011.

Liu, H. and Z. Liu. (2010). Recycling utilization patterns of coal mining waste in China. *Resources Conservation and Recycling*. **54**, 1331-1340.

Majdar, R. S., and H. Ghassemian. (2017). A probabilistic SVM approach for hyper spectral image classification using spectral and texture features. *International Journal of Remote Sensing*. **38**, 4265-4284.

Ng, K. H., Y. W. Cheng, Z. S. Lee, M. R. Khan, S. S. Lam, and C. K. Cheng. (2018). Experimental evaluation and empirical modelling of palm oil mill effluent steam reforming. *International Journal of Hydrogen Energy*. **43**, 15784-15793.

Nkwuda NG, Theophine MA, Okogwu OI (2019). Impacts Of Rock Mineralization And Poor Sanitary System On Borehole Waters Quality And The Health Implications. *Earth Sciences Pakistan*, 10-13.

Ogunkunle, Joseph T, Adewumi, Aderiike, Adepoju, Olufemi A (2019). Biodiversity: Overexploited but Underutilized Natural Resource for Human Existence and Economic Development. *Environment & Ecosystem Science*, **3,** 26-34.

Qi, B., C. Zhao, and G. Yin. (2014). Feature weighting algorithms for classification of hyper spectral images using a support vector machine. *Applied Optics*. **53**, 2839.

Sana B, Haroon R, Abdul N, Rana A N (2019). Spatial And Temporal Variability Analysis Of PM2.5 Concentration In Lahore City. *Environmental Contaminants Reviews*, **2,** 6-10.

Singh, A. and P. Raj. (2019). Sustainable recycling model for municipal solid waste in Patna. *Energy & Environment*. **30**, 212-234.

Slavkovikj, V., S. Verstockt, W. D. Neve, et al. (2016). Unsupervised spectral sub-feature learning for hyper spectral image classification. *International Journal of Remote Sensing*. **37**, 309-326.

Szopa, A., and H. Ekiert. (2014). Production of biologically active phenolic acids in Aronia melanocarpa, (Michx.) Elliott in vitro cultures cultivated on different variants of the Murashige and Skoog medium. *Plant Growth Regulation*. **72**, 51-58.

Tang, X.Y., K. Gao, and G.Q. Ni. (2014). Hyper spectral unmixing based on nonlinear dimensionality reduction. *Computer Simulation*. **31**, 347-351.

Varela, C. E., E. Fromentin, and M. Roller, et al. (2016). Effects of a natural extract of aronia melanocarpa berry on endothelial cell nitric oxide production. *Journal of Food Biochemistry*. **40**, 404.

Zhang, J., X.W. Zhu, and Y. He. (2012). Application of hyper spectral remote sensing images classification method. *Computer Simulation*. **29**, 281-284.

Zhou, Y., and Y. Wei. (2016). Learning hierarchical spectral-spatial features for hyper spectral image classification. *IEEE Transactions on Cybernetics*. **46**, 1667-1678.